Laboratory synthesized calcium oxide and calcium hydroxide grains: A candidate to explain the 6.8 μm band

Yuki Kimura and Joseph A. Nuth III

Astrochemistry Laboratory, Code 691, Solar System Exploration Division, NASA's Goddard Space Flight Center, Greenbelt, MD 20771, USA

Abstract

We will demonstrate that CaO and $Ca(OH)_2$ are excellent candidates to explain the 6.8 μm feature, which is one of the most obscure features in young stellar objects. We discuss the condensation of CaO grains and the potential formation of a $Ca(OH)_2$ surface layer. The infrared spectra of these grains are compared with the spectra of fifteen young stellar objects. We note that CaO-rich grains are seen in all meteoritic CAIs (calcium-aluminum-rich inclusions) and the 6.8 μm feature has only been observed in young stellar objects. Therefore, we consider CaO grains to be a plausible candidate to explain the 6.8 μm feature and hypothesize that they are produced in the hot interiors of young stellar environments.

1. Introduction

Many grains are formed through condensation from the gas phase after mass ejection from evolved stars. Most of these grains are eventually incorporated into new protostellar systems either after their initial destruction and alternation by supernova shock waves and galactic cosmic rays in the interstellar medium or after passing through the interstellar medium (ISM) and becoming incorporated into cold molecular cloud cores. The galaxy has countless numbers of protostellar systems in various evolutionary stages. The behavior of protostellar systems more massive than the solar nebula has been observed and used to probe evolutionary processes that might apply to our solar system.

Protostellar objects have several significant infrared features and many kinds of materials have been proposed as candidates to account for those features. For example, hydrogenated amorphous carbon (e.g. Brooke, Sellgren & Smith 1996), polycyclic aromatic hydrocarbons (Bregman & Temi 2001) and ammonia in ice (Dartois et al. 2002) have all been proposed as candidates to explain the band at 3.46-3.49 μm. It has also been proposed that CH_3OH can account for the 3.54 μm band (e.g. Brooke, Sellgren & Smith 1996), that an organic residue is responsible for the band at 6.0 μm (e.g. Gibb & Whittet 2002) and that the 9.7 and 18 μm bands are due to amorphous silicate (e.g. Schutte et al. 1998; Gibb et al. 2004). In this paper, we will concentrate on the band observed at 6.8 μm, which is one of the most obscure features in young stellar objects.

The 6.8 μm feature attracted considerable interest after it was first discovered in young stellar objects (Russell et al. 1977). Recently, even though high-resolution spectra were obtained by the Short Wavelength Spectrometer (SWS) attached to the Infrared Space Observatory (ISO) (Dartois et al. 1999; Keane et al. 2001), the carrier of the 6.8 μm feature still remains unidentified. Several kinds of materials have been proposed to explain this feature, including C-H deformation modes (Gibb et al. 2004), NH_4^+ (e.g. Grim et al. 1989, Demyk et al. 1998) and H_2CO (Schutte et al. 1996). However each of these candidates requires very specific environmental conditions to explain the observations, e.g. Why is the feature only seen in protostars and not in the cold molecular cloud phase?

The identification of any feature requires a careful comparison of the infrared spectra observed in the astrophysical objects and spectra obtained in the laboratory, including spectra of synthetic analogues of plausible candidates. For various reasons, detailed below, we believe that complex of CaO and $Ca(OH)_2$ could be a reasonable candidate to explain observations of a 6.8 μm feature in protostellar systems. An experimental apparatus, designed to make large quantities of highly amorphous, well mixed smoke grains from the gas phase is frequently used in our laboratory (Nelson et al. 1989). We believe that these smokes are comparable to cosmic condensates. Here we report the laboratory synthesis of CaO grains using this apparatus and a comparison of the infrared spectra of these grains to the observed protostellar spectra near 6.8 μms.

2. Experimental procedure

Calcium oxide and calcium silicate smoke grains were prepared in the laboratory by vapor phase condensation using the Condensation Flow Apparatus (Nelson et al. 1989; Nuth, Rietmeijer & Hill 2002). The grains were then annealed in vacuum in a manner that could potentially correspond to the thermal evolution of protostellar dust particles evaporated near the protostar and recondensed in the bipolar outflow.

Since astronomical conditions cannot be exactly duplicated, the laboratory samples are simple analogs of more complex materials that might be found in natural systems. Smoke grains were produced at a total pressure of ~80 Torr in an atmosphere dominated by hydrogen at temperatures between 1080 and 1170 K. The hydrogen flow rate was always ~500 sccm (standard cubic centimeters per minute). Calcium metal (Alfa Aesar, A Johnson Matthey Company, 99%) was placed into a graphite boat inside an alumina furnace tube. At the nominal 1080 K temperature of the furnace, calcium metal has a vapor pressure of ~1 Torr. An eight to ten minute run produced about 1 g of white smoke. Six samples of calcium oxide grains with varying degrees of oxidation were produced in six different experimental runs carried out using oxygen flow rates that varied between 30 and 400 sccm and several different furnace temperatures. The samples had colors that varied from white to gray as the degree of oxidation decreased. For the production of calcium silicate smokes SiH_4 gas was added to the gas mixture at the same flow rate as was used for the oxygen.

The total pressure was again controlled to ~80 Torr, the same pressure used to produce the calcium oxide smokes.

Annealing experiments were performed on 7.5-mg smoke samples in alumina ceramic tubes at total pressures less than 4×10^{-5} atm. and at oven temperatures of 900, 1027, 1100, 1200 and 1300 K. Infrared spectra of the samples, embedded in KBr pellets, were measured with a Fourier-transform infrared spectrometer (Mattson Polaris FT-IR spectrometer). The infrared system utilized a KBr beam splitter and deuterated triglyceride sulfate detector. The wavelength resolution used for this work was 2 cm^{-1}.

Both the condensed and annealed smoke samples were mounted on holey amorphous carbon thin films supported by standard 200-mesh Cu TEM grids. Transmission electron microscope (TEM) observations were carried out using a JEOL 2010 TEM operated at an accelerating voltage of 200 keV at the University of New Mexico. The TEM was equipped with an ultra-thin window energy-dispersive X-ray analysis system for in situ quantitative chemical analysis of very small grains such as interplanetary dust particles (IDPs) that are typically similar to the size of the CaO grains or smaller.

3. Results and discussion

The smoke grains can be classified by their colors: they were white, light gray and dark gray. These colors correspond to the degree of oxidation of calcium. The white smoke grains are well oxidized, i.e., most of the grains

are CaO. On the other hand, the dark gray specimens are less oxidized, i.e., metallic calcium grains with surface oxide coatings are dominant. Light gray grains are somewhere between those two grain types.

Figure 1 shows the mid-infrared spectra of those three type grains. The three spectra have a similar characteristic absorption feature centered at 6.8 μm, independent of the color of the specimens. The intensity of the 6.8 μm band does seem to depend on the degree of oxidation, i.e., the intensity of the 6.8 μm band observed in the white CaO smokes becomes weaker as the color of the grains becomes darker. This effect can easily be explained by the total amount of CaO versus Ca metal in each smoke grain: the ratio depends on the conditions under which the grains were synthesized.

In the case of the white grains, the calcium oxide smokes are produced directly from the vapor phase from calcium and oxygen. The reaction occurs between atomic calcium and oxygen near the evaporation source. After formation of CaO molecules, they grow by coalescence of the small CaO clusters in the gas flow. As a result, homogeneous calcium oxide smoke grains are produced. In the case of the light gray grains, the calcium metal could begin nucleating directly over the carbon boat before extensive reaction with the oxygen gas: this could result from a lower oxygen flow rate or from a high vapor pressure of the calcium metal in the experiment. When the calcium metal grains contact oxygen gas, oxidation occurs on the surface of the calcium metal grains. Since the grains are extremely small, most, but not all, of the calcium metal grains react to form CaO grains. Figure 2 shows a typical TEM image and the corresponding electron diffraction pattern of the

condensed calcium oxide grains of light gray color. Many small voids are visible in the TEM image of the grain. These voids are typically produced by the oxidation of metallic particles after exposure to air (Kaito, Fujita & Hashimoto 1973). Therefore, this TEM image strongly supports the growth process discussed above. In the case of the gray grains, the calcium metal grains are only lightly oxidized due to the high calcium/oxygen ratio and calcium oxides are formed only on the surfaces of the grains. The gray color is a reflection of the remaining calcium metal. Therefore, we conclude that the intensity of the 6.8 μm band of the gray grains is weak due to a high ratio of Ca metal (neutral extinction)) to CaO. On the other hand, the peak position of the 6.8 μm band is observed to be independent of the degree of oxidation, as would be expected.

It is known that CaO reacts with water to form $Ca(OH)_2$. Since the size of the analog CaO grains are on the order of nanometers, they have an enormous surface to volume ratio. Therefore, they easily react with moisture upon exposure to air. In order to elucidate the effect of water on CaO grains, the spectra of $Ca(OH)_2$ grains were measured. Figure 3 shows a mid-infrared spectrum of $Ca(OH)_2$ grains produced from white CaO grains dispersed in water. Three characteristic features at 6.11, 6.85 and 11.5 μm, which can be also seen in the spectra of CaO grains (shown in Fig. 1) are visible. $Ca(OH)_2$ was not observed during TEM analysis, as shown in Fig. 2. Therefore, $Ca(OH)_2$ is probably produced only as a few nanometer thick coating on the surface of the CaO grains. Since nanometer sized grains have a lot of surface area, even if the $Ca(OH)_2$ layer is only a few nanometers

thick, the most significant features of this coating material will appear in the infrared spectrum. Therefore, we conclude that the dual peak centered near 6.8 μms and a small peak at 11.5 μm in the spectra of our CaO grains are produced by bulk absorption in CaO combined with absorption by a $Ca(OH)_2$ layer on the surface of the CaO grains. If the $Ca(OH)_2$ layer is not formed, then the 6.8 μm band becomes a single narrow peak. Unfortunately, the infrared spectra of completely dry CaO grains were never observed in these experiments due to fast reaction of the tiny grains with the atmosphere.

In addition to the 6.8 and 11.5 μm bands, a very narrow peak at 2.7 μm, a small bump at 9.2 μm, and an increase in absorption intensity toward longer wavelengths were also observed in the spectra of CaO grains. Since the intensity of the 2.7 μm feature decreased after annealing in air, we attribute this feature to oxygen defects in the CaO grains. The 9.2 μm bump is nearly coincident with the strongest absorption feature of amorphous silicate. Figure 4 shows a mid-infrared spectrum of calcium silicate smoke grains. In addition to the 6.8 μm feature originating from CaO, the strong 9.2 μm feature attributed to amorphous silicate can be also observed. As a result of energy-dispersive X-ray analysis of the CaO grains, the atomic ratio of the silicon in our specimens was found to be less than 1 %. Since this value is within our experimental measurement error, it cannot be known whether or not the CaO samples actually contain silicon as a contaminant. However, these CaO grains were produced using same apparatus used for the production of calcium silicate smokes. Accordingly,

very small amounts of silicon oxide may contaminate the products of these experiments and account for the presence of a feature at 9.2 μm.

Since bulk crystalline CaO has a strong absorption feature at ~21.7 μm (Millar & Duley, 1978), an increase in the absorption intensity toward longer wavelengths in the infrared spectra of CaO grains might be attributed to the bulk absorption of CaO crystals. Indeed, the absorption intensity of CaO grains became stronger at longer wavelength as annealing at 900-1300 K induced crystallization and growth of the CaO grains. Even then, the peak position at 6.8 μm did not change. CaO grains found in CAIs are on the order of 100-200 nm (Greshake et al. 1996), which is coincident with the size of our analog CaO grains. We conclude that the absorption feature originating from CaO grains is responsible for the main band observed at 6.8 μm and that those from $Ca(OH)_2$ grains produce the 6.85 and 11.5 μm features.

Figure 5 shows mid-infrared spectra ranging from 5 to 8 μm obtained using the SWS on the ISO for fifteen young stellar objects observed by Gibb and colleagues (Gibb et al. 2004). The mid-infrared spectra of CaO and $Ca(OH)_2$ grains are also shown at the bottom of both columns. The peak positions of the 6.8 μm feature in these young stellar objects range from approximately 6.56 to 6.95 μm which is coincident with the peak positions in our CaO grains. However, the 6.8 μm feature of the analog CaO grains is somewhat broader than those seen in the most of young stellar objects. The main reason for the width of the feature is the $Ca(OH)_2$ surface layer on the CaO grains. A secondary reason might be an imperfect match of the analog

grains to the size distribution and shape of the natural CaO grains. The profile of the infrared feature is affected by the size, shape and structure of the grain. Since production of smoke grains using our experimental apparatus is chaotic, smoke samples are composed of grains of various sizes and shapes. The infrared spectra from 5 to 30 μm for Mon R2 IRS2, which has widest 6.8 μm feature, is shown in Fig. 6. The profile of the 6.8 μm feature of Mon R2 IRS2 is quite similar to that of CaO grains including $Ca(OH)_2$. Moreover, the intensity of the11.5 μm feature of Mon R2 IRS2 is significantly stronger than those of other sources seen in Fig. 6. Therefore, we suggest that the 6.8 μm band of Mon R2 IRS2 is produced by CaO and $Ca(OH)_2$ which can easily be produced by the reaction between CaO grains and water vapor in the young stellar environment.

Although several kinds of materials have been proposed to explain the 6.8 μm feature, including C-H deformation modes (Gibb et al. 2004), NH_4^+ (e.g. Grim et al. 1989, Demyk et al. 1998), H_2CO (Schutte et al. 1996), these candidates all require specific conditions for their formation process and should be observed in the spectra of cold molecular cloud cores. Additionally, several other features attributable to those candidates should also be observed in the spectra from natural systems. More recently proposed candidates for the 6.8 μm feature are complex high-molecular-weight organic materials. However, their formation in young stellar environments becomes more difficult to explain as their molecular weight increases.

We note that the 6.8 μm band is composed of very close dual peaks as seen in Fig. 1 which is produced by a $Ca(OH)_2$ layer on the CaO grains.

Astronomical 6.8 μm features may also consist of these two components as well. Therefore we propose that observers might test our hypothesis by obtaining careful measures of the shape of the 6.8 μm band and/or by searching for the weaker 11.5 μm feature in protostellar sources.

Although the 6.8 μm feature is observed in young stellar objects, it has not been observed in either the interstellar medium or in circumstellar outflows around evolved stars. Moreover, CaO grains do not condense under equilibrium conditions (Greshake et al. 1996). However, CaO grains are seen in all CAIs, characteristic components of carbonaceous chondrites that must have been produced in the solar nebula. Shu et al. (1996) have proposed that CAIs could form in the high temperature x-region of protostars. CaO grains could be produced in such a high temperature environment, close to the protostars that show the 6.8 μm feature. Therefore, we believe that CaO grains (together with $Ca(OH)_2$ coatings of varying thickness) are a plausible candidate to explain the 6.8 μm features seen in young stellar objects.

Acknowledgements

TEM analysis was performed in the Electron Microbeam Analyses Facility of the Department of Earth and Planetary Sciences at the University of New Mexico, where Adrian J. Brearley and Ying-Bing Jiang provided technical support. This work was partially supported by grants from JSPS Postdoctoral Fellowships for Research Abroad from April 2004 to March 2006.

References

Bregman, J. D., & Temi, P. 2001, ApJ, 554, 126.

Brooke, T. Y., Sellgren, K., & Smith, R. G. 1996, ApJ, 459, 209.

Dartois, E., Demyk, K., d'Hendecourt, L., & Ehrenfreund, P. 1999, A&A, 351, 1066.

Dartois, E., d'Hendecourt, L., Thi, W., Pontoppidan K. M., & van Dishoeck, E. F. 2002, A&A, 394, 1057.

Demyk, K., Dartois, E., d'Hendecourt, L., Jourdain de Muizon, M., Heras, A. M., & Breitfellner, M. 1998, A&A, 339, 553.

Gibb, E. L., & Whittet, D. C. 2002, ApJ, 566, 113.

Gibb, E. L., Whittet, D. C. B., Boogert A.C.A., & Tielens, A.G.G.M. 2004, ApJS, 151, 35.

Greshake, A., Bischoff, A. Putnis, A., & Palme, H. 1996, Meteoritics & Planetary Science, 31, A54.

Grim, R. J. A., Greenberg, J. M., de Groot, M. S., et al. 1989, A&AS, 78, 161.

Kaito, C., Fujita, K., & Hashimoto, H. 1973, Jpn. J. Appl. Phys., 12, 489.

Keane, J. V., Tielens, A. G. G. M., Boogert, A. C. A., Schutte, W. A., & Whitter, D. C. B. 2001, A&A, 376, 254.

Millar, T. J., Duley, W. W. 1978, MNRAS, 183, 177.

Nelson, R., Thiemens, M., Nuth, J., & Donn, B. 1989, Proc. Lunar Planet. Sci. Conf., 19th, 559.

Nuth, J. A., Rietmeijer, F. J. M., & Hill, H. G. M. 2002, Meteoritics & Planetary Science, 37, 1579.

Russell, R. W., Soifer, B. T., & Puetter, R. C. 1977, A&A, 54, 959.

Schutte, W. A., Gerakines, P. A., Geballe, T. R., van Dishoeck, E. F., & Greenberg, J. M. 1996, A&A, 309, 633.

Schutte, W. A., et al. 1998, A&A, 337, 261.

Shu, F. H., Shang, H., & Lee, T. 1996, Science, 271, 1545.

Figure caption

Figure 1. Mid-infrared spectra of calcium oxide smoke samples.

Figure 2. Typical TEM image and the corresponding ED pattern of light gray CaO smoke grains.

Figure 3. Mid-infrared spectra of calcium hydroxide ($Ca(OH)_2$) smoke samples.

Figure 4. Mid-infrared spectra of calcium silicate smoke samples.

Figure 5. Mid-infrared spectra from 5 to 8 μm for fifteen young stellar objects that were observed by Gibb and colleagues (Gibb, et al., 2004). The mid-infrared spectra of our analog CaO and $Ca(OH)_2$ grains are also shown at the bottom of both columns.

Figure 6. Comparison of the mid-infrared spectra of three typical young stellar objects with our laboratory grains over the range from 5 to 30 μm.

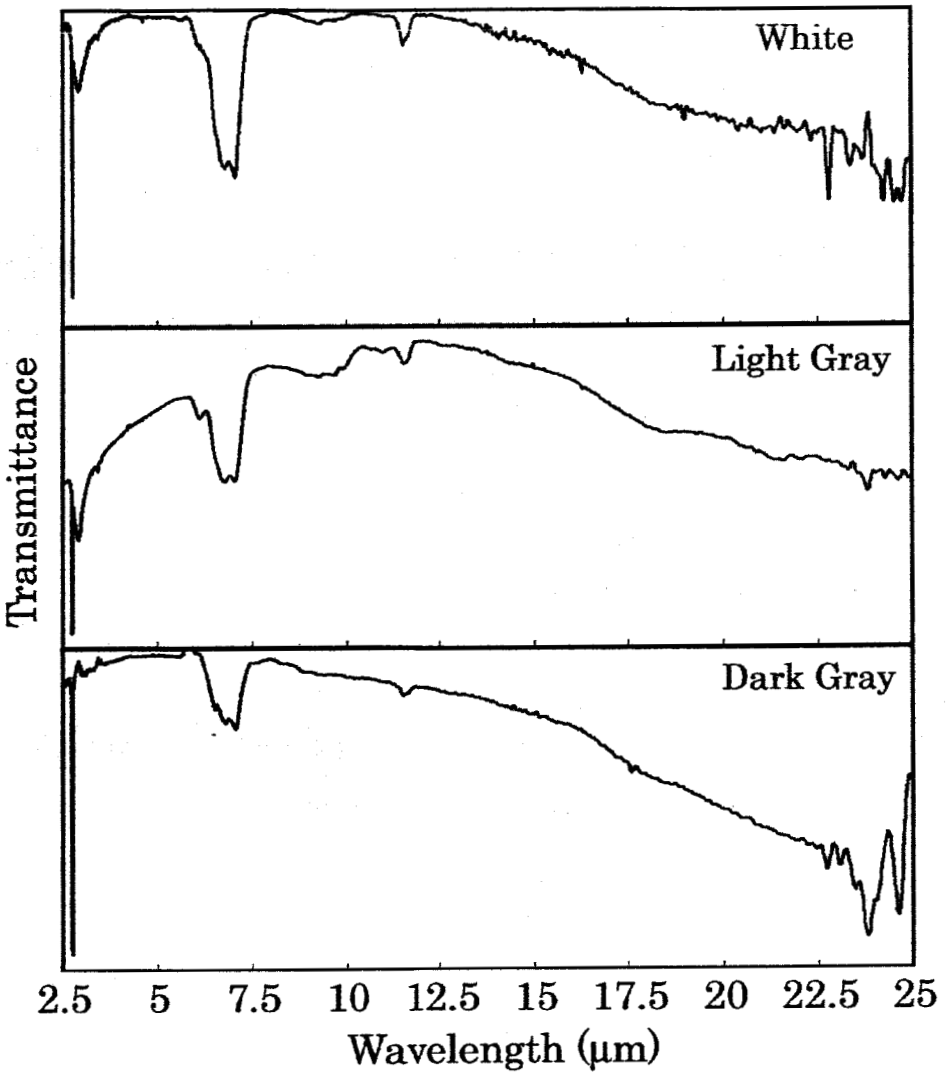
White
Light Gray
Dark Gray
Transmittance
2.5
5
7.5
10
12.5
15
17.5
20
22.5
25
Wavelength (μm)

Fig. 1

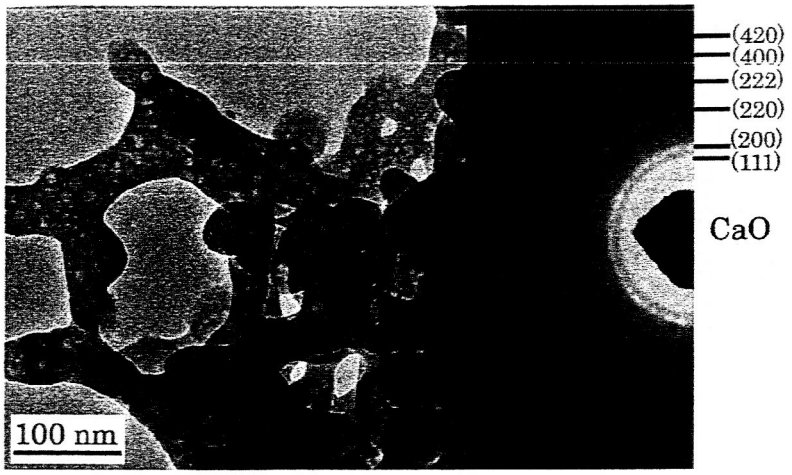
(420)
(400)
(222)
(220)
(200)
(111)
CaO
100 nm

Fig. 2

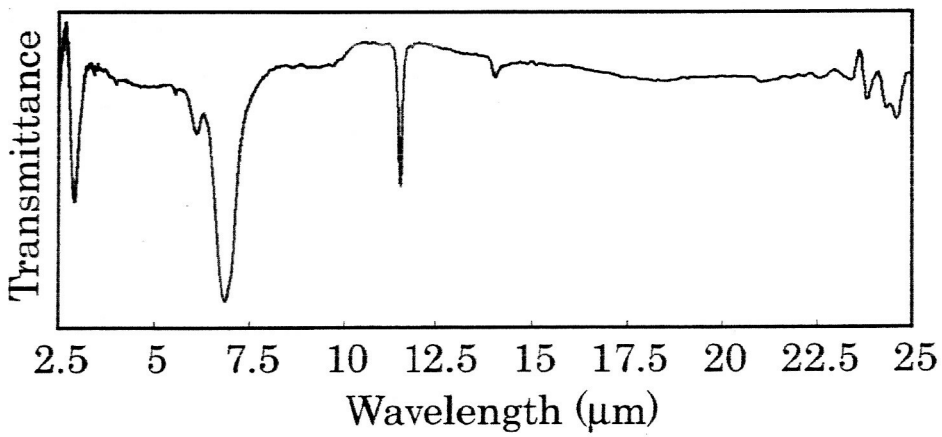
Transmittance
2.5
5
7.5
10
12.5
15
17.5
20
22.5
25
Wavelength (μm)

Fig. 3

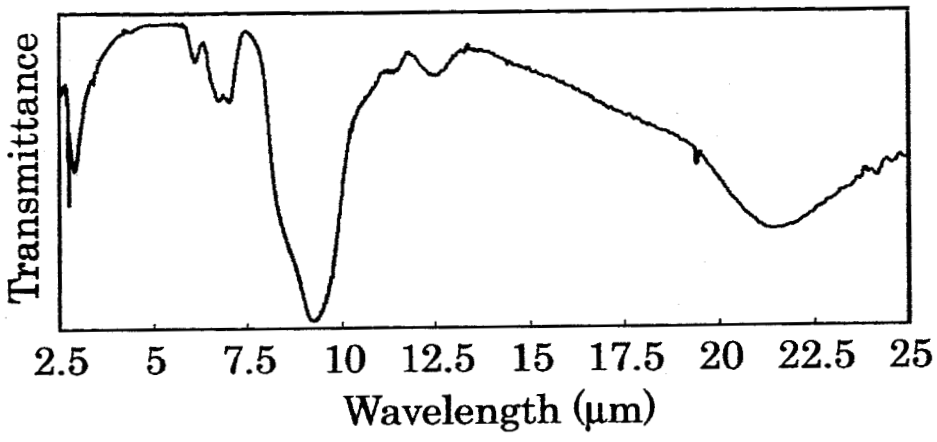

Fig. 4

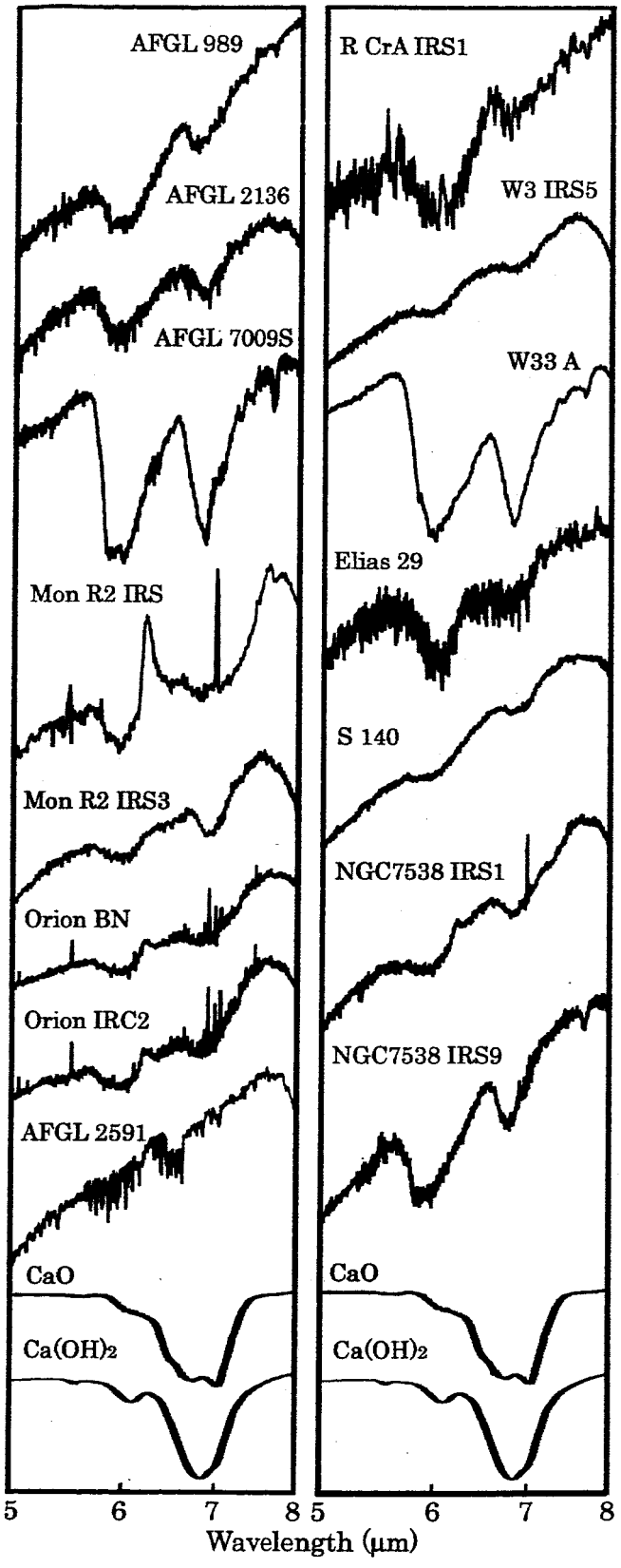
AFGL 989
AFGL 2136
AFGL 7009S
Mon R2 IRS
Mon R2 IRS3
Orion BN
Orion IRC2
AFGL 2591
CaO
Ca(OH)2
R CrA IRS1
W3 IRS5
W33 A
Elias 29
S 140
NGC7538 IRS1
NGC7538 IRS9
CaO
Ca(OH)2
5
6
7
8
5
6
7
8
Wavelength (μm)

Fig. 5

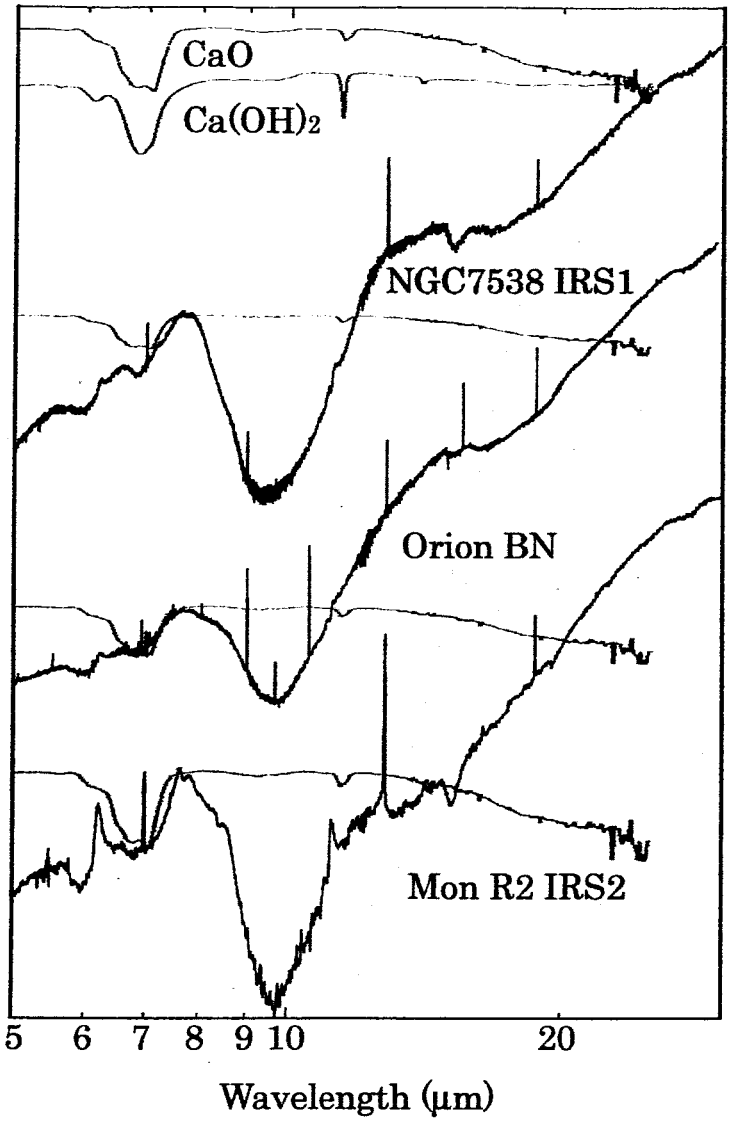
CaO
Ca(OH)2
NGC7538 IRS1
Orion BN
Mon R2 IRS2
5
6
7
8
9
10
20
Wavelength (μm)

Fig. 6